Dispersion field analysis using discrete wavelet transform for inter-turn stator fault detection in induction motors

H. Cherif, A. Menacer, Raphael Romary, Remus Pusca

▶ **To cite this version:**

H. Cherif, A. Menacer, Raphael Romary, Remus Pusca. Dispersion field analysis using discrete wavelet transform for inter-turn stator fault detection in induction motors. 2017 IEEE 11th International Symposium on Diagnostics for Electrical Machines, Power Electronics and Drives (SDEMPED), Aug 2017, Tinos, France. pp.104-109, 10.1109/DEMPED.2017.8062341 . hal-04383947

HAL Id: hal-04383947

https://univ-artois.hal.science/hal-04383947

Submitted on 9 Jan 2024

HAL is a multi-disciplinary open access archive for the deposit and dissemination of scientific research documents, whether they are published or not. The documents may come from teaching and research institutions in France or abroad, or from public or private research centers.

L'archive ouverte pluridisciplinaire **HAL**, est destinée au dépôt et à la diffusion de documents scientifiques de niveau recherche, publiés ou non, émanant des établissements d'enseignement et de recherche français ou étrangers, des laboratoires publics ou privés.

Dispersion field analysis using Discrete Wavelet Transform for inter-turn stator fault detection in Induction Motors

H. Cherif, A. Menacer
Electrical Engineering Laboratory of Biskra, Biskra University, Algeria
hakima.hakima5@gmail.com, menacer_arezki@hotmail.com

R. Romary, R. Pusca
Univ. Artois, EA 4025 LSEE, F-62400, Béthune, France
raphael.romary@univ-artois.fr, remus.pusca@univ-artois.fr

***Abstract*—This paper presents an inter-turn short circuit detection through the measurement of external magnetic field of induction motor. The technique of analysis is based on discrete wavelet transform energy in transient state where the machine operates at start-up and standstill states. The wavelet offers a very fine analysis of the unidimensional and two-dimensional signals. Through multilevel discrete wavelet decomposition, it is possible to extract the information for the prognosis of the fault in variable state of the machine. The stored energy calculation in each decomposition can evaluate the severity of the fault compared with the analysis of only the external magnetic field.**

Keywords – Induction machine, inter turns short circuit fault, magnetic field, diagnosis, energy, discrete wavelet transform.

I. INTRODUCTION

Diagnostic Methods based on the analysis of external magnetic field have been developed since the end of the 70's [1] and they have been improved by better modelling of the external magnetic field of electrical machines in faulty conditions [2]. These methods have been proved to be able to detect stator faults, rotor faults, or mechanical faults [3-5]. Their main advantages are the non-invasive investigation, and the simplicity of implementation. Moreover, it has been shown that these methods are more sensitive then MCSA especially for inter-turn short circuit fault [6].

The analysis generally uses data picked up from external flux sensors when the machine operates at standstill, and then the FFT allows extracting sensitive harmonics from the signal. When a high frequency resolution is required, a long acquisition time during standstill operation of the machine is necessary, but in some case it is not possible because the load imposes fast speed or torque variations. In this case, non stationary signal processing tools, like Short Time Fourier Transform, wavelets, or Wigner Ville distribution are more convenient [7], [8].

The aim of this paper is to exploit data obtained from an external flux sensor during a direct line start up of an induction machine in case of an inter-turn short circuit fault. It can be expected that this transient highlight the effect of the fault. In this paper we will analyse the energy obtained from the external magnetic field analysis using DWT in order to detect the fault in case of direct line start-up and during standstill states.

The paper is organized as follows: in the next section basis on the external magnetic field are presented, then the discrete wavelet transform is introduced, finally experimental results are presented.

II. THE EXTERNAL MAGNETIC FIELD

A. Presentation

The external magnetic field results from an axial and a transverse component obtained from leakage fluxes created by the different elements of the machine [9]. The axial field is in a lengthwise plan that includes the machine axis. This field is mainly generated by the currents flowing in the end winding of the stator. The transverse field is located in a plan perpendicular to the machine axis. This field is directly tied to the air-gap flux density *b* which is attenuated by the stator iron.

According to the position of the sensor, the measured field does not come from the same source, and does not result from the same physical phenomenon. Therefore, the measured signal will be sensitive to different field components and it will depend on the position of the sensor around the machine periphery. In Fig.1 the different positions of the coil sensor are illustrated. Regarding the path of the field lines, the sensor placed in Pos. 2 measures the axial field. In Pos. 3 it measures only the radial field in Pos. 3 because in that position, the sensor is parallel with the lengthwise plan of the machine, and the linked flux of the sensor concerned by the axial field is null. In Pos. 1 the sensor measures the radial field but also a part of the axial field.

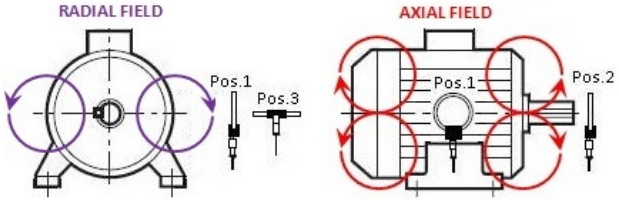

Fig.1 External field measurement

B. Theoretical approach

The analysis of the external magnetic field is based on the radial field and it requires to model the air gap flux density b. This latter can be written using

the general equation obtained from the fourier series decomposition of internal magnetic variables:

$$b = \sum_{K,H} \hat{B}_{K,H} \cos\left(K\omega t - H\alpha^s - \varphi_{K,H}\right) \quad (1)$$

α^s is the angular position of any point relatively to a stator spatial reference axis d^s tied to the phase 1 axis. The magnitude $\hat{B}_{K,H}$ depends on the supply current harmonics, the stator and rotor space harmonics, and the slotting effect. K is the frequency rank and H is the pole pair number of the flux density component; for a healthy machine, these ranks are defined as [10]:

$$\left.\begin{aligned} K &= 1 + krN^r(1-s) \\ H &= p(h^s + ksN^s + krN^r) \end{aligned}\right\} \quad (2)$$

Where h^s is the mmf rank that takes all the values defined by: h^s=6k+1 (k varies between -∞ to +∞). *ks* and *kr* are permeance ranks, that are positive, negative or null integers. s is the slip of the induction machine and N^s, N^r are respectively the number of stator slots and rotor bars per pole pair.

In case of a stator inter-turn short circuit, additional components of ranks K_{sc} and H_{sc} appear. They are defined as:

$$\left.\begin{aligned} K_{sc} &= 1 + kr'N^r(1-s) \\ H_{sc} &= h + p(ks'N^s + kr'N^r) \end{aligned}\right\} \quad (3)$$

ks' and *kr'* are equivalent to *ks* and *kr*, they vary from -∞ to + ∞. h is a non-null relative integer, which can take consequently all the values of h^s. h is tied to the rank of the mmf generated by the faulty turns flowed through by the short circuit current.

Equations (2) and (3) point out that the K and K_{sc} ranks take the same values. On the other hand, H is multiple of p whereas H_{sc} can take 1 as lowest value.

The harmonic components of b at $K\omega$ or $K_{sc}\omega$ angular frequency will be found in the radial field after attenuation by the stator iron. Let us point out that the radial flux density at any point M outside the machine of polar coordinates x, α^s can be decomposed in a normal and a tangential component, respectively b_n and b_t as shown in the simplified geometry given in Fig. 2. It is assumed that the considered machine has a smooth air gap where the flux density given by (1) is imposed. Fig. 2 also gives the position of the sensor, placed at the level of the point M.

Let denotes b^x the normal transverse flux density at radius x= R^s_{ext}. b^x is defined as :

$$b^x = \sum_{K,H} C_H \hat{b}_{K,H} \cos\left(K\omega t - H\alpha^s - \varphi_{K,H}\right)$$

The attenuation coefficient related to the stator yoke, denoted by C_H, depends on the inner and outer radius of the stator laminations, respectively R^s_{int} and R^s_{ext}, and the magnetic permeability μr [10]. It has been shown that C_H, can be expressed as:

$$C_H = \frac{2}{\mu r\left((R^s_{\text{int}}/R^s_{ext})^{-|H|-1} - (R^s_{\text{int}}/R^s_{ext})^{|H|-1}\right)}$$

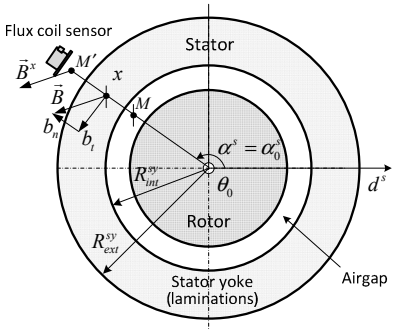

Fig. 2. Simplified geometry of the machine

Fig.3 shows the evolution of C_H versus H for $R^s_{\text{int}} = 82.5$ mm, $R^s_{\text{ext}} = 121$mm and μr=1000. It can be observed that the more H increases, the more the components are attenuated.

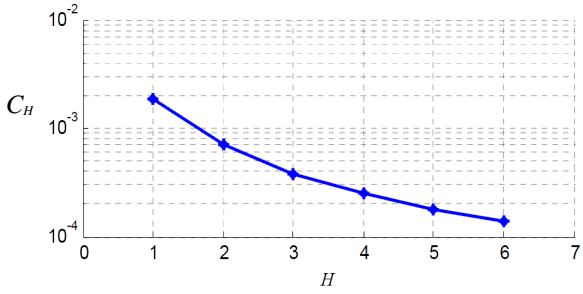

Fig. 3. C_H versus H

As mentioned earlier, for a healthy machine, the polarity H is multiple of the machine pole pair number. For a faulty machine, the dissymmetry produced by the fault leads to the generation of additional flux density components such that H_{sc}=1. These components are not strongly attenuated by the stator iron and they are highlighted in the external magnetic field. This property makes the analysis of this variable interesting compared with current analysis. Moreover, in the case of an inter-turn short circuit fault, the short circuit current produces its own magnetic effect that will be refund in the external magnetic field, and less attenuated than the supply current.

III. DISCRETE WAVELET TRANSFORM (DWT)

The DWT is a powerful technique in a wide range of engineering and scientific applications and can be implemented efficiently with filter banks (FB) [11].

The filter bank has a regular structure; it is easily implemented by repeated application of identical

cells. It is also computationally efficient [12]. The basic idea behind decomposition is low-pass and high-pass filtering with the use of down sampling and up sampling respectively. It results that wavelet decomposition is a hierarchically organized decomposition. One can choose the level of decomposition *j* based on a desired cutoff frequency.

Fig. 4 shows an implementation of a three-level forward DWT based on a two-channel recursive filter bank, where *g(n)* and *h(n)* are low-pass and high-pass analysis filters, respectively and provide diagnosis information in two frequency bands. A_j is the low-frequency approximation [13] and D_j is the high-frequency detail signal, both at resolution *j*.

$$D_j^k = \sum_n g_{n-2k}\, A_{j-1}^k \tag{4}$$

$$A_j^k = \sum_n H_{n-2k}\, A_{j-1}^k \tag{5}$$

Where $A_0(k)$ is the original signal. After decomposing the signal, it's obtained one approximation signal A_j and D_1, D_2 ,..., D_j detail signals [14].

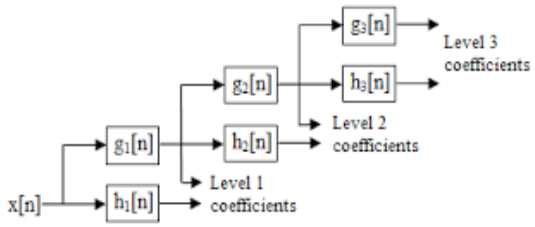

Fig. 4. *The DWT decomposition of a signal*

The energy eigen value for each frequency band is defined by [15]:

$$E_j = \sum_{k=1}^{k=n} \left| D_{j\,k}(n) \right|^2 \tag{6}$$

Such as *j* is the level of decomposition.

The eigenvalues of the energy levels of the decomposition signal contain information tied to the state of the machine; and the line of these values can be used to diagnose and to identify the degree of fault. The deviation of certain inherent value indicates the severity of the defect [15].

IV. Experimental Results

A. Experimental test bench

The experiments are done for a three phase induction motor: 11 kW, 4 poles**.** The machine parameters are given in the appendix. This machine has been rewound so that each elementary section is brought back to an external connection box. This allows one to short circuit a full elementary section, what corresponds to 12.5% of a full phase winding. The short circuit current can be limited through a rheostat.

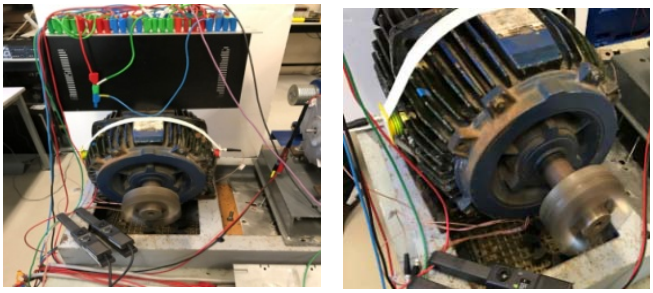

Fig 5. *Motor of the tests equipped with 2 wound sensors placed outside of the machine*

In this study, the short circuit fault diagnosis and detection is carried out from the external magnetic flux analysis. The latter is measured using a wound sensor with a surface area **S** and having ***n*** turns. This one is placed on the side of the machine, at equal distance of the extremities of the breech [6], as shown in Fig.5.

This test bench offers the possibility to observe the behavior of the motor in start-up and standstill states in healthy state and with 12.5% short circuit of one phase winding. The short circuit current is adjusted at 5A and 10A through the external rheostat. The energy obtained for different harmonics components by analysis of external magnetic field using DWT is expected to provide information about the presence of the fault. Different signals delivered by the wound sensor are picked up:

- at start-up for the healthy machine, and for an inter-turn short circuit fault (5A and 10A),
- at stand-still for the healthy machine and for an inter-turn short circuit fault (5A and 10A).

As an example, Fig 6 shows the start up signal in healthy case and for a 10A short circuit.

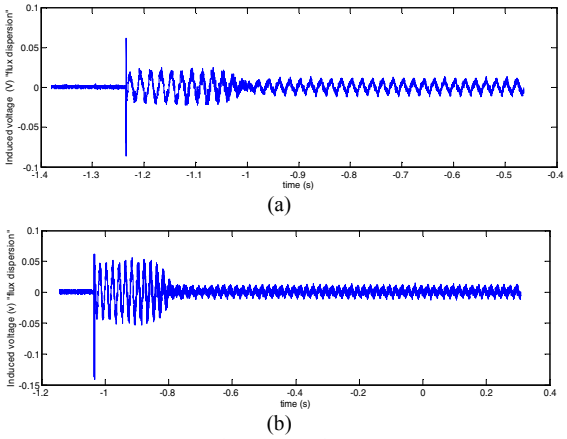

Fig. 6. *Signal at start up:*
(a) healthy machine –(b) faulty machine with 10A short circuit current

B. DWT analysis

Before the application of the DWT, it's necessary to select the type of mother wavelet and the number of decomposition levels. There is no absolute way to choose a certain wavelet. The choice of wavelet

depends upon the type of signal to be analyzed and the application. There are several wavelet families like Haar, Daubechies, Biorthogonal, Coiflets, Symlets, Morlet, Mexican Hat, Meyer [13]. In our case, Daubechies (Db44) wavelet it's chosen for extracting the fault components of the short circuit effect in two cases: start-up and standstill. The number of decomposition level is done by:

$$n_{ls} \succ \text{int}\left(\frac{\log\left(\frac{f_e}{f_s}\right)}{\log(2)}\right) + 1 \qquad (7)$$

where:

n_{ls}: number of decomposition levels
f_e=25 kHz: the sampling frequency of the signal being analyzed.
f_s = 50 Hz: the fundamental frequency of the signal being analyzed.

Therefore the range of real frequency components of the signals is between 0 and 25000 Hz. Table I gives the correspondence between DWT coefficients and range of frequencies.

The analysis of external magnetic field in start-up and standstill states is realized by the calculation of the energy of the detail decomposition for different cases: healthy and short circuit fault (5A and 10A). Results are presented in Fig.7.

Table I: *Frequency bands for the wavelet signal*

Level	Frequency bands Approximation (Hz)		Frequency bands Details (Hz)	
J=1	A1	0-12500	D1	12500-25000
J=2	A2	0-6250	D2	6250-12500
J=3	A3	0-3125	D3	3125-6250
J=4	A4	0-1562.5	D4	1562.5-3125
J=5	A5	0-781.25	D5	781.25-1562.5
J=6	A6	0-390.625	D6	390.625-781.25
J=7	A7	0-195.3125	D7	195.3125-390.625
J=8	A8	0-97.6563	**D8**	**97.6563-195.3125**
J=9	A9	0-48.8281	**D9**	**48.8281-97.6563**
J=10	A10	0-24.4141	D10	24.4141-48.8281
J=11	A11	0- 12.2070	D11	12.2070-24.4141
J=12	**A12**	**0-6.1035**	**D12**	**6.1035-12.2070**

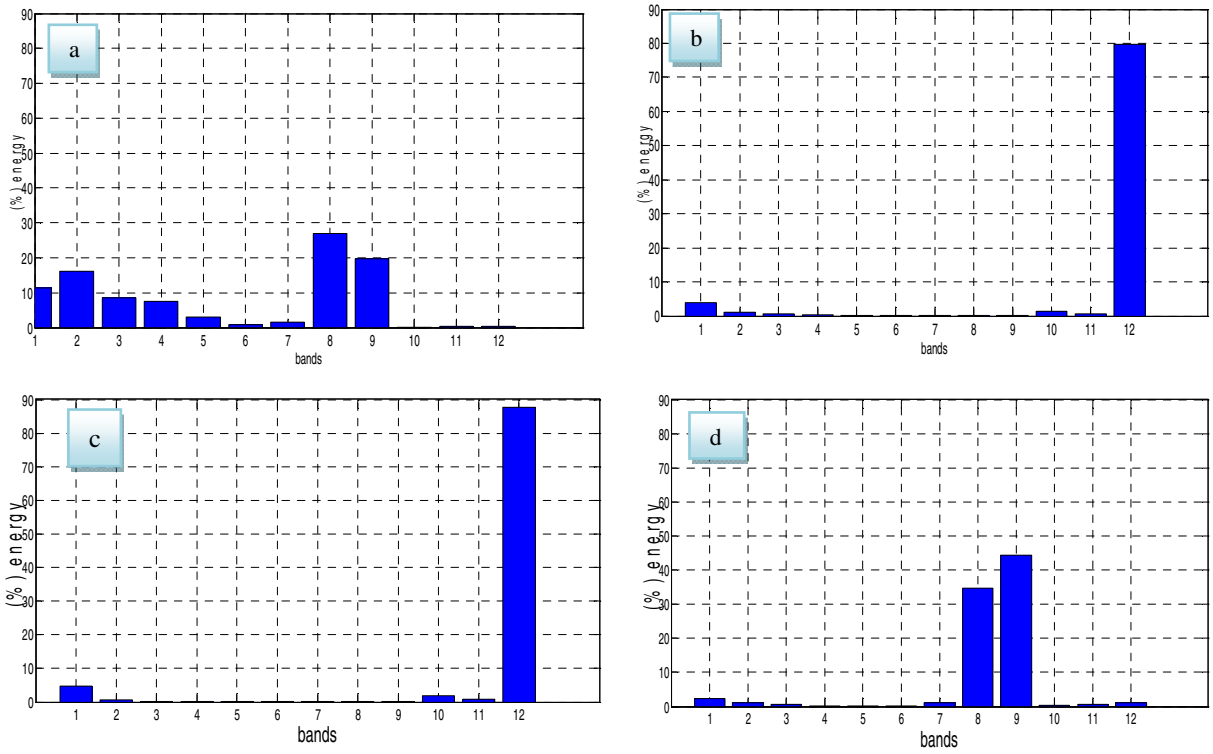

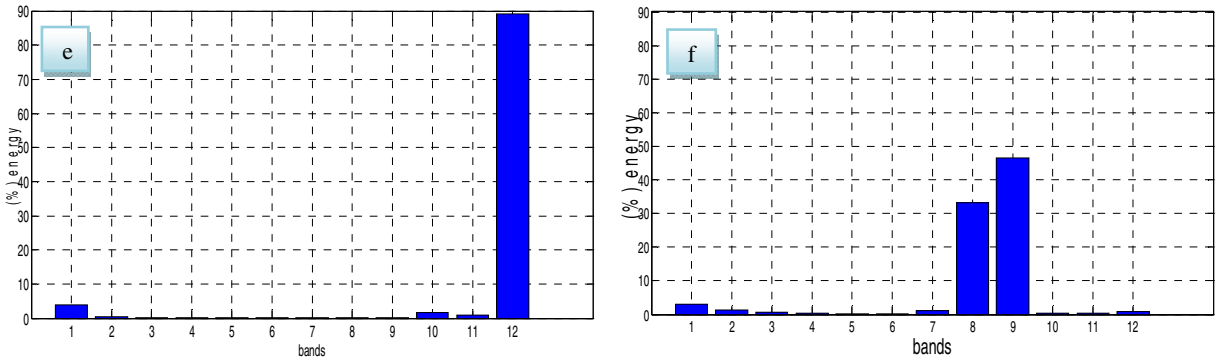

Fig.7: *Variation of energy in frequency bands at start-up and standstill states*:

***a**: Start-up state with healthy state, **b**: Standstill state with healthy state*
***c**: Start-up state with short circuit faults (5A), d: Standstill state with short circuit faults (5A)*
*e: Start-up state o with short circuit faults (10A)**, f**: Standstill state with short circuit faults (10A)*

Table II: *Summary of results*

	Start-up			Standstill		
	DWT Coefficients Indicator	**Percentage of energy (EDWT%)**	**Frequency bands (Hz)**	**DWT Coefficients indicator**	**Percentage of energy (EDWT%)**	**Frequency bands (Hz)**
Healthy state	**D8** **D9**	**13%** **43%**	**[97.6563-195.3125]** **[48.8281-97.6563]**	**D12**	**79.77%**	**[6.1035-12.2070]**
inter turn short circuit fault with 5A	**D12**	**87.7%**	**[6.1035-12.2070]**	**D8** **D9**	**34.67%** **44.42%**	**[97.6563-195.3125]** **[48.8281-97.6563]**
inter turn short circuit fault with 10A	**D12**	**89.19%**	**[6.1035-12.2070]**	**D8** **D9**	**33.20%** **46.47%**	**[97.6563-195.3125]** **[48.8281-97.6563]**

Table. II shows the recapitulation of the figure 7 results showing the variation of the energy of the detail coefficient with frequency bands for the healthy and short circuit fault of the machine at start-up and standstill state. It is observed that the values of the energy are different in each case. Therefore, on can choose the best coefficient as fault indicator.

It can be observed that in healthy case (fig. 7.a and 7.b), for the start-up state, the stored energy value increases slightly for the level of detail decomposition D8 and D9, while in standstill state a considerable increase in detail D12 (79.77% of total energy) is observed.

Fig. 7 (c, d, e and f) show the variation of the energy for two cases of short-circuit fault (5A, 10A) at start-up and standstill.

For the start-up state, it is clear that the value of detail D12 has been increased considerably (**89.19%** for the 10A fault and **87.7%** for the 5A fault). The level of increase depends on the degree of short circuit defect.

The fault effect is very clear in the energy level compared with healthy state of the machine at start-up state. The energy in the level D12 increases significantly and the energy in the levels D8 and D9 decreases compared with the healthy state of the machine.

For the standstill state , the inter turn short circuit fault does not reveal the fault severity (5A or 10A) compared with the analysis at start-up state of the machine.

V. Conclusion

In this paper, a inter-turn short circuit fault detection is considered by external magnetic field analysis using discrete wavelet transform in transient state, when the machine operate in start-up and standstill state. The technique of diagnosis is based on energy evaluation of the external magnetic field. The inter turn short circuit fault severity is more visible in start-up state compared with standstill state of the machine, especially for the both defects (5A, 10A).

The wavelet energy is able to extract useful characteristics from the external magnetic on the non stationary regime of the machine.

VI. Appendix

Parameters of the machine:

P_n: Output power	11KW
V_s: Stator voltage	400/230V
I_s: Nominal current	17/23A
N_n: Nominal speed	1425 rpm
f_s: Stator frequency	50Hz
P: Number of Pole pairs	2
N_r: Number of stator slots	48
n_b: Number of rotor bars	32
n_s: Number of turn per stator phase	256

VII. References

[1] P.J. Tavner, P. Hammond, J. Penman, "Contribution to the study of leakage fields at the ends of rotating electrical machines", IEE, Vol. 125, N°12, 1978, pp.1339-1349.

[2] M. Barzegaran, A. Mazloomzadeh, O.A. Mohammed, "Fault diagnosis of the asynchronous machines through magnetic signature analysis using finite-element method and neural networks", *IEEE Trans. on Energy Conversion*, vol. 28, pp. 1064-1071,October 2013.

[3] H. Henao, C. Demian, and G.A. Capolino, "A frequency-domain detection of stator winding faults in induction machines using an external flux sensor", *IEEE Trans. Ind. Appl.*, vol. 39, pp. 1272–1279, Sept/Oct. 2003.

[4] A. Ceban, R. Pusca, and R. Romary, "Study of rotor faults in induction motors using external magnetic field analysis", *IEEE Trans. Ind. Electron.*, vol. 59, pp. 2082-2093, May 2012.

[5] L. Frosini, C. Harlisca, L. Szabo, "Induction Machine Bearing Fault Detection by Means of Statistical Processing of the Stray Flux Measurement", *IEEE Trans. Ind. Electron.*, vol. 62, no. 3, pp. 1846-1854, March 2015.

[6] R. Romary, R. Corton, D. Thailly, and J. F. Brudny, "Induction machine fault diagnosis using an external radial flux sensor", *The European Physical Journal - Applied Physics,* vol. 32, pp. 125-132, 2005.

[7] H. Douglas, P. Pillay, A.K. Ziarani, "A new algorithm for transient motor current analysis using wavelets". IEEE trans. on Industry Applications, vol. 40, N° 5, Sept. 2004, pp. 1361-1368.

[8] M. Blodt, J. Faucher, B. Dagues, M. Chabert, "Mechanical load fault detection in induction motors by stator current time-frequency analysis", IEEE International Electric and Drives Conference IEMDC 2005, San Antonio, Texas USA, May 2005. pp. 1881-1888

[9] R. Romary, D. Roger, J.F. Brudny. "Analytical computation of an AC machine external magnetic field", European Physical Journal-Applied Physics EPJ-AP, EDP Sciences, Paris, Vol. 47, N°3 Paper 31101, Sept. 2009.

[10] J. D. Thailly, R. Romary, D. Roger, J.F. Brudny, "Attenuation of magnetic field components through an AC machine stator", COMPEL, Vol. 27, No. 4, 2008, pp.744-753

[11] Selvaraaju Murugesan, David B.H. Tay, "A new class of almost symmetric orthogonal Hilbert pair of wavelets", Signal Processing 95 (2014) 76– 87

[12] Olivier Rioul and Pierre Duhamel, "Fast algorithms for discrete and continuous wavelet transforms", IEEE Transactions on information theory,Vol. 38, No. 2, March 1992.

[13] Rachid HADDADI, Elhassane ABDELMOUNIM, Mustapha EL HANINE, " Discrete wavelet transform based algorithm for recognition of QRS complexes", World of Computer Science and Information Technology Journal (WCSIT), ISSN: 2221-0741, Vol. 4, No. 9, 127-132, 2014.

[14] Ahcène Bouzida, Omar Touhami, Rachid Ibtiouen, "Fault diagnosis in industrial induction machines through discrete wavelet transform", IEEE Transactions on Industrial Electronics, Vol. 58, No. 9, September 2011.

[15] H. Cherif, A. Menacer, B. Bessam, and R.Kechida, "Stator inter turns fault detection using discrete wavelet transform", 2015 IEEE 10th International Symposium on Diagnostics for Electrical Machines Power Electronics and Drives (SDEMPED), 2015.